

VectorFit : Adaptive Singular & Bias Vector Fine-Tuning of Pre-trained Foundation Models

Suhas G. Hegde¹ Shilpy Kaur¹ Aruna Tiwari¹

Abstract

Popular PEFT methods achieve parameter efficiency by assuming that **incremental weight updates are inherently low-rank**, which often leads to a performance gap compared to full fine-tuning. While recent methods have attempted to address this limitation, they typically lack sufficient parameter and memory efficiency. We propose VectorFit, an effective and easily deployable approach that **adaptively trains the singular vectors and biases** of pre-trained weight matrices. We demonstrate that the utilization of structural and transformational characteristics of pre-trained weights enables high-rank updates comparable to those of full fine-tuning. As a result, VectorFit achieves superior performance with $9\times$ less trainable parameters compared to state-of-the-art PEFT methods. Through extensive experiments over 17 datasets spanning diverse language and vision tasks such as natural language understanding and generation, question answering, image classification, and image generation, we exhibit that VectorFit consistently outperforms baselines, even in extremely low-budget scenarios.

1. Introduction

Pre-trained foundation models (PFMs) have set unprecedented standards in language, vision, and audio tasks (Touvron et al., 2023; Rombach et al., 2021; Radford et al., 2022), showcasing their strong performance across diverse domains. Refining these models through fine-tuning is a powerful approach to enhance their performance across diverse downstream tasks (Li et al., 2023; Yu et al., 2024). This process helps models adhere to given instructions (Xu et al., 2024a), adopt preferred behaviors, and discard undesirable ones (Rafailov et al., 2023). However, adapting these models to downstream tasks through full fine-tuning

¹Department of Computer Science & Engineering, Indian Institute of Technology Indore. Correspondence to: Suhas G. Hegde <>.

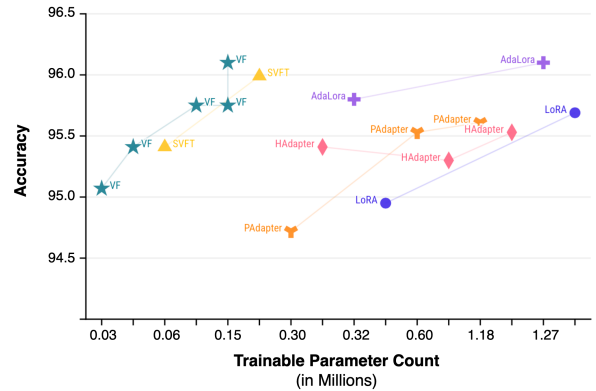


Figure 1: Accuracy vs Trainable parameter count for SST2 dataset. VectorFit (labeled as VF for brevity) outperforms baselines with 85% less trainable parameters. The graph highlights that VectorFit is a PEFT method in extremely low parameter regime of $<0.1\%$ trainable parameters.

(Full-FT) is a significant challenge, primarily due to the immense computational and memory overhead. For instance, models like DeBERTa-V3 (He et al., 2023) with 300 million parameters, ViT-22B (Dehghani et al., 2023) with 22 billion parameters, and Llama-3 (Grattafiori et al., 2024) with a staggering 405 billion parameters exemplify the scale of modern PFMs. Adapting these models for multiple downstream tasks is resource-intensive and typically requires maintaining separate copies of the full model for each task, leading to a very high memory consumption.

Parameter-Efficient Fine-Tuning (PEFT) mitigates these challenges by introducing a small set of trainable parameters to produce specialized models. For example, PFMs like LLMs are fine-tuned for tasks such as text classification (Wang et al., 2019), question answering (Rajpurkar et al., 2016), and text generation (Li et al., 2021) using task-specific datasets. PEFT techniques, such as LoRA (Hu et al., 2021) and adapter (Pfeiffer et al., 2021), significantly reduce the number of trainable parameters compared to Full-FT, although this can sometimes compromise performance. More advanced methods like AdaLoRA (Zhang et al., 2023b) try to increase expressiveness by adaptively choosing trainable

parameters, bridging the performance gap. However, majority of successful PEFT methods rely on the assumption that incremental weight matrices are low-rank, which limits their expressiveness and disregards the nuances of weight matrix transformation during Full-FT. Moreover, even state-of-the-art PEFT techniques (e.g., LoRA, Adapter, and AdaLoRA) can still result in a substantial number of trainable parameters, even in their highest parameter-efficient setup (e.g., LoRA with rank 1). Although there are a few recent methods that do not rely on low-rank updates (Qiu et al., 2023; Lingam et al., 2024), all of them, to the best of our knowledge, work based on fine-tuning a newly initialized set of weight matrices. This leads to a high overall parameter count and memory consumption, twice as that of LoRA in SVFT (Lingam et al., 2024).

This prompts the question: Can we achieve high-rank adaptation without incurring prohibitive parameter and memory costs? As an answer, we introduce VectorFit, which directly leverages the structural and transformational characteristics of the pre-trained weights instead of introducing new weights for fine-tuning, differentiating our method from prior work. Given a pre-trained weight matrix W_0 , VectorFit applies singular value decomposition (SVD), such that $W_0 = U\Sigma V^T$. The method then selectively adapts the singular vector (Σ) and the bias (b) associated with W_0 , focusing on those Σ and b that exhibit suboptimal training compared to those of other weight matrices. We propose a mechanism called *Adaptive Vector Freezing* to achieve this.

Since the singular vectors represent the stretching of the weight matrices in their high-dimensional subspace, directly fine-tuning them allows for high expressiveness (Appendix D.5). Additionally, training the bias vectors gives translational degree of freedom, further enhancing the expressiveness during fine-tuning.

Hence, VectorFit performs high-rank updates comparable to Full-FT (Figure 9) while using significantly fewer trainable parameters ($\leq 0.1\%$). It outperforms the baselines in terms of performance relative to parameter efficiency (Figure 1). VectorFit also shows a practical memory consumption approximately equivalent to that of LoRA with rank 1 (Figure 5).

2. Related Work

Researchers have explored three primary approaches to reduce the number of parameters required for fine-tuning while preserving or enhancing the performance of PFMs. These approaches can be broadly categorized into Adapter-based methods, LoRA-based methods, and other PEFT methods.

Adapter-Based methods. This research direction emphasizes incorporating small neural networks into PFMs and

fine-tuning only these modules for specific tasks, keeping the base model frozen and shared across tasks. This approach introduces a limited number of task-specific parameters, significantly improving the scalability and practicality of large models. For instance, adapter tuning (Houlsby et al., 2019; Pfeiffer et al., 2021; He et al., 2022) integrates small neural networks, known as adapters, between the layers of the base model. Other methods, such as prefix tuning (Li & Liang, 2021) and prompt tuning (Lester et al., 2021), add trainable prefix tokens to the input or hidden layers of the model. These techniques claim to have demonstrated performance comparable to Full-FT while updating less than 1% of the model parameters, significantly reducing memory requirements.

LoRA-Based methods. A significant advancement in PEFT is Low-Rank Adaptation (LoRA) (Hu et al., 2021), which preserves the pre-trained model weights and incorporates trainable low-rank matrices within each transformer layer. For a pre-trained weight matrix $W_0 \in \mathbb{R}^{d_r \times d_c}$, LoRA constrains the weight update ΔW to a low-rank decomposition: $y = W_0x + \Delta Wx = W_0x + BAx$, where $B \in \mathbb{R}^{d_r \times r}$, $A \in \mathbb{R}^{r \times d_c}$ and rank $r \ll \min(d_r, d_c)$. Only A and B are trainable parameters.

Several studies have introduced variations of the LoRA algorithm, focusing on reducing the number of trainable parameters (Zhang et al., 2024a; Kopiczko et al., 2024; Ding et al., 2023), improving the flexibility of low-rank structures (Koochpayegani et al., 2024; Zi et al., 2024; Sun et al., 2024), enabling adaptive parameter allocation (Zhang et al., 2023a), and integrating LoRA with techniques like quantization (Dettmers et al., 2024; Xu et al., 2024b) and pruning (Zhang et al., 2024b).

A significant enhancement over LoRA is AdaLoRA (Zhang et al., 2023b), which addresses LoRA’s limitation of evenly distributing trainable parameters across weight matrices, ignoring their varying importance. In AdaLoRA, the incremental updates are parameterized as singular value decomposed matrices $P\Lambda Q$, where $P \in \mathbb{R}^{d_r \times r}$ and $Q \in \mathbb{R}^{r \times d_c}$ are the left and right singular matrices, $\Lambda \in \mathbb{R}^{r \times 1}$ is the singular vector. The orthogonality of P and Q is maintained using the regularizer $R(P, Q) = \|P^T P - I\|_F^2 + \|QQ^T - I\|_F^2$. The rank of low-rank updates is dynamically adjusted using an importance metric derived from Λ . By pruning less significant singular values while allowing for recovery, AdaLoRA claims to have improved performance with a similar parameter budget as LoRA.

Other PEFT methods. Orthogonal Fine-Tuning (OFT) (Qiu et al., 2023) introduces an orthogonal projection approach using orthogonal regularization. It focuses on optimizing parameters while preserving the orthogonality of weight updates, ensuring minimal interference with pre-trained knowledge. However, it still demands a signifi-

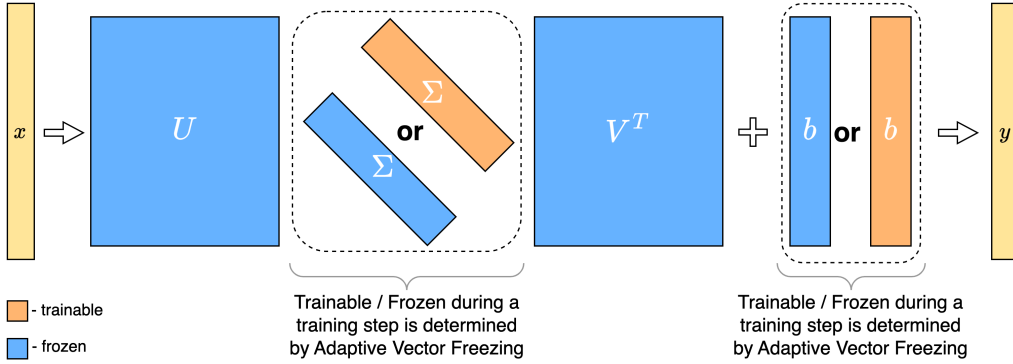


Figure 2: Architecture diagram of VectorFit. The pretrained weight matrix is initially decomposed into U , Σ , and V . Subsequently, only Σ and bias b are trained with Adaptive Vector Freezing mechanism.

cant number of trainable parameters because of the high dimensionality of the matrices. Butterfly Orthogonal Fine-Tuning (BOFT) (Liu et al., 2024) builds upon OFT by introducing Butterfly factorization and claims to improve parameter efficiency, and fine-tuning flexibility. Singular Vectors guided Fine-Tuning (SVFT) (Lingam et al., 2024) leverages the singular value decomposition of pre-trained weight matrices to parameterize weight updates as $y = W_0x + \Delta Wx = U(\Sigma + M)V^Tx$, where M is a sparse trainable matrix with pre-determined and fixed sparsity pattern. As M is not restricted to be low-rank, SVFT claims to achieve high-rank gradient updates. Nonetheless, SVFT uses four matrices, U , Σ , V , and M , for every pre-trained weight matrix. Also, their dimensions are comparable to those of the pre-trained weight matrix. This leads to a high parameter and memory cost. On the other hand, VectorFit is an SVD-based PEFT method that directly trains the singular and bias vectors in a selective manner, significantly reducing the overall parameter and memory cost.

3. VectorFit

In this section, we describe VectorFit and its components in detail. VectorFit comprises two key components: (1) Vector Fine-Tuning, based on SVD. (2) *Adaptive Vector Freezing*, a mechanism to avoid co-adaptation and to improve the performance.

3.1. Vector Fine-Tuning

VectorFit initially performs SVD on the pre-trained weight matrix $W_0 \in \mathbb{R}^{d_r \times d_c}$, such that, $W_0 = U\Sigma V^T$. W_0 can be the weight matrix of any of the modules in self-attention (q, k, v, o) or multilayer perceptron (f_1, f_2) of a transformer block. Then we potentially fine-tune only the singular vector Σ and the pre-trained bias vector b_0 corresponding to W_0 , subject to *Adaptive Vector Freezing*, as shown in Figure 2. Formally, this can be denoted as follows:

$$y = (U\Sigma V^T)x + b_0 \quad (1)$$

where $x \in \mathbb{R}^{d_{in} \times d_r}$ is the input hidden state. $U \in \mathbb{R}^{d_r \times d_r}$ is the left singular matrix and $V \in \mathbb{R}^{d_c \times d_r}$ is the right singular matrix of W_0 , consisting of orthonormal column vectors. V^T is the transpose of V . $\Sigma \in \mathbb{R}^{d_r \times 1}$ and $b_0 \in \mathbb{R}^{d_c}$ are the potentially trainable singular vector and bias vector of W_0 , respectively. $y \in \mathbb{R}^{d_{out} \times d_c}$ is the output hidden state. Note that Σ in standard SVD is a diagonal matrix and we store it as a vector for memory efficiency. The weight updates of VectorFit are parameterized as:

$$W = W_0 + \Delta W = U(\Sigma + \Delta\Sigma)V^T \quad (2)$$

$$b = b_0 + \Delta b \quad (3)$$

where ΔW , $\Delta\Sigma$, and Δb are the incremental matrix/vectors of W_0 , Σ , and b_0 , respectively.

Singular values of a weight matrix quantify the scaling factors for the transformation along its orthogonal directions, an important aspect of the weight matrix. Directly fine-tuning them as described above results in an overall high-rank incremental matrix whose rank is comparable to that of full fine-tuning of the weight matrix. This is analyzed in detail in Section 6.2.

To avoid performing the expensive calculation of SVD for every single pre-trained weight matrix during each training step, we perform SVD in the beginning of the fine-tuning and replace the original weight matrices of the model with their decomposed version. This takes a few seconds of extra time in the beginning of the fine-tuning, which is negligible. Although this approach increases the total parameter count—for instance, VectorFit with DeBERTaV3-base has 18% more parameters than LoRA ($r = 1$) with DeBERTaV3-base—its practical training memory consumption remains

similar to LoRA ($r = 1$). More details on this is given in Appendix A.

3.2. Adaptive Vector Freezing

As we train only a small number of parameters (a few tens of singular and bias vectors), it is crucial to ensure balanced training across all trainable vectors. This prevents some vectors from being over-trained while others remain under-trained, a phenomenon known as co-adaptation.

To address this, we propose *Adaptive Vector Freezing (AVF)*, a mechanism that periodically freezes (disables the gradients of) the top- k trainable vectors that have undergone extensive training. This allows the remaining under-trained vectors to receive adequate updates. The extent of training of each vector is quantified in the form of training strength. Consider the set of all trainable vectors, $V = \{\Sigma_{l,m}, b_{l,m} : l = \text{layer}, m = \text{module}(q, k, v, o, f_1, f_2)\}$. We define the training strength $S_v(t)$ of a vector $v \in V$ at training step t as L1 norm between v_0 and v_t , formulated as follows:

$$S_v(t) = \frac{1}{\text{dim}(v)} \|v_0 - v_t\|_1 \quad (4)$$

where v_0 is the value of v before fine-tuning and v_t is the value of v during the training step t . $\text{dim}(v)$ is the dimension of v . To find the top- k vectors, we perform exponential moving average of $S_v(t)$ as given in Eq. 5.

$$S'_v(t) = \beta S'_v(t - t_f) + (1 - \beta) S_v(t) \quad (5)$$

where $\beta = 0.99$, is a constant. We define the training step at which AVF is applied as the AVF step. Given the frequency of AVF steps t_f , the first AVF step t_i , the number of vectors k to freeze per AVF step, and the total number of AVF steps n_f , the top- k vectors with the highest $S'_v(t)$ values are frozen at each AVF step. Note that the trainability of vectors do not change in between AVF steps. However, a vector frozen during one AVF step may become trainable in a subsequent AVF step, ensuring that all vectors are adequately trained over time. More details on these hyperparameters are given in Appendix C.

In Section 6.1, we theoretically and experimentally show that this mechanism leads to similar results as that of dropout. It is important to note that using the standard dropout algorithm for singular vectors results in a significant performance drop, even with a very low dropout probability. This signifies that certain singular values, and their corresponding left and right singular directions are extremely important that they cannot be dropped. Therefore, the AVF mechanism is crucial for maintaining effective training.

4. Experiments

Implementation details. All algorithms are implemented using PyTorch (Paszke et al., 2019). Our implementation builds upon the publicly available Huggingface Transformers codebase (Wolf et al., 2020). Appendix C contains the full details of our experimental setup and hyperparameter configurations.

4.1. Tasks and Datasets

We evaluate our method on the following tasks and datasets:

1. Natural Language Understanding (NLU): Experiments are conducted on the GLUE benchmark (Wang et al., 2019), which includes single-sentence classification, similarity/paraphrase, and natural language inference tasks.
2. Question Answering (QA): Performance is tested on SQuAD v1.1 and SQuAD v2.0 (Rajpurkar et al., 2016), treating QA as a sequence labeling problem to predict the start and end token probabilities for answer spans.
3. Natural Language Generation (NLG): Evaluation is performed on the XSum (Narayan et al., 2018) and CNN/DailyMail (Nallapati et al., 2016) datasets for text summarization task.
4. Image Classification: Our method is assessed on image classification tasks using CIFAR10 (Krizhevsky, 2009), GTSRB (Stallkamp et al., 2012), MNIST (Deng, 2012), and RESISC45 (Cheng et al., 2017) datasets.
5. Image Generation: The results on subject-driven image generation is evaluated using the Dreambooth dataset (Ruiz et al., 2023).

4.2. Base Models

We use four distinct base model types that are representative of a wide range of PFMs for the evaluation of our algorithm:

1. DeBERTaV3-base (He et al., 2023), a transformer encoder-only language model, applied to NLU and QA tasks.
2. BART-large (Lewis et al., 2020), a transformer encoder-decoder model, used for NLG tasks.
3. ViT-base (Dosovitskiy et al., 2021), a vision transformer model, applied to image classification tasks, pre-trained on Imagenet-1K.
4. Stable Diffusion v1.4 (Rombach et al., 2021), a latent diffusion model based on UNet architecture, used for text-to-image generation.

Table 1: DeBERTaV3-base fine-tuned using various PEFT methods is evaluated on the GLUE benchmark. For performance metrics, we report matched accuracy for MNLI, Matthew’s correlation for COLA, Pearson correlation for STS-B, and accuracy for the other tasks, where higher values indicate better performance across all metrics. # Params is the number of trainable parameters.

Method	# Params	MNLI	SST2	COLA	QQP	QNLI	RTE	MRPC	STSB
Full FT	184M	89.90/90.12	95.63	69.19	92.40/89.80	94.03	83.75	89.46	91.60
HAdapter	1.22M	90.13/90.17	95.53	68.64	91.91/89.27	94.11	84.48	89.95	91.48
PAdapter	1.18M	90.33/90.39	95.61	68.77	92.04/89.40	94.29	85.20	89.46	91.54
LoRA(r=8)	1.33M	90.65/90.69	94.95	69.82	91.99/89.38	93.87	85.20	89.95	91.60
AdaLora	1.27M	90.76/90.79	96.10	71.45	92.23/89.74	94.55	88.09	90.69	91.84
HAdapter	0.61M	90.12/90.23	95.30	67.87	91.65/88.95	93.76	85.56	89.22	91.30
PAdapter	0.60M	90.15/90.28	95.53	69.48	91.62/88.86	93.98	84.12	89.22	91.52
HAdapter	0.31M	90.10/90.02	95.41	67.65	91.54/88.81	93.52	83.39	89.25	91.31
PAdapter	0.30M	89.89/90.06	94.72	69.06	91.40/88.62	93.87	84.48	89.71	91.38
LoRA(r=2)	0.33M	90.30/90.38	94.95	68.71	91.61/88.91	94.03	85.56	89.71	91.68
AdaLora	0.32M	90.66/90.70	95.80	70.04	91.78/89.16	94.49	87.36	90.44	91.63
SVFT	0.28M	89.90/89.97	95.99	72.61	91.50/88.98	93.90	88.09	88.99	91.73
VectorFit	0.15M	<u>90.12/89.89</u>	96.10	<u>70.94</u>	<u>91.51/88.70</u>	<u>94.05</u>	<u>84.12</u>	92.16	91.76

Baselines. We compare our approach against Full-FT, which updates all parameters across all layers. Additionally, we evaluate it against state-of-the-art methods from each of the three categories mentioned in Section 2. These include LoRA (Hu et al., 2021), AdaLoRA (Zhang et al., 2023b), PAdapter (Pfeiffer et al., 2021), HAdapter (Houlsby et al., 2019), and SVFT (Lingam et al., 2024).

5. Results

In the tables, the highest accuracy within each trainable parameter count regime is highlighted in **bold**, and the overall parameter efficiency (% accuracy / % trainable parameters) is reported with underline.

5.1. Natural Language Understanding

Table 1 presents the results on the GLUE benchmark, where VectorFit outperforms Full-FT by an average of 0.6% while requiring over 1200× fewer trainable parameters. Its performance is comparable to baselines like LoRA (r = 8), which uses 9× more trainable parameters. VectorFit outperforms SVFT by upto 3.2% with 2× less parameters. Notably, VectorFit achieves the highest parameter efficiency across all datasets in the GLUE benchmark, establishing it as the most optimal PEFT method for natural language understanding tasks.

5.2. Question Answering

We evaluate the performance of our method on the SQuAD v1.1 and the more challenging SQuAD v2.0 datasets, using exact match (EM) and F1 scores as metrics. The results, summarized in Table 2, demonstrate that VectorFit outperforms the baselines on SQuAD v1.1 giving 0.9% better F1 score on an average. It achieves superior results compared to Full-FT with 1250× fewer parameters. On SQuAD v2.0, VectorFit delivers performance comparable to Full-FT and the best-performing baselines, highlighting its efficiency and effectiveness.

Table 2: Performance results for DeBERTaV3-base fine-tuned on SQuAD v1.1 and SQuAD v2.0 are presented. # Params indicates the percentage of trainable parameters. The metrics reported are Exact Match and F1 scores (EM/F1).

Model	Squad v1.1 (EM/F1)	Squad v2.0 (EM/F1)
Full FT	86.0 / 92.7	85.4 / 88.4
# Params	0.08%	0.08%
HAdapter	84.4 / 91.5	83.4 / 86.6
PAdapter	84.4 / 91.7	84.2 / 87.2
LoRA	86.4 / 92.8	84.6 / 87.5
AdaLora	86.8 / 93.0	84.7 / 87.6
SVFT	86.3 / 92.5	84.3 / 87.3
VectorFit	87.0 / 93.2	84.4 / 87.6

Table 3: Performance results for BART-large fine-tuned on the XSum and CNN/DailyMail datasets are shown. The # Params column represents the percentage of trainable parameters. The reported metrics are ROUGE-1, ROUGE-2, and ROUGE-L (R-1/2/L).

Method	# Params	Xsum	CNN/Dailymail
Full FT	100%	45.49 / 22.33 / 37.26	44.16 / 21.28 / 40.90
PAdapter	0.16%	40.21 / 18.92 / 32.34	41.96 / 19.47 / 38.10
LoRA	0.16%	42.81 / 19.68 / 34.73	43.68 / 20.63 / 40.71
AdaLoRA	0.16%	43.29 / 19.95 / 35.04	43.94 / 20.83 / 40.96
SVFT	0.15%	43.30 / 19.82 / 35.13	43.87 / 20.72 / 40.80
VectorFit	0.12%	43.28 / 20.71 / 35.42	44.01 / 21.60 / 40.98

Table 4: The performance results for ViT-base fine-tuned on the CIFAR10, GTSRB, MNIST, and RESISC45 datasets are presented. The # Params column indicates the proportion of trainable parameters, and the corresponding image classification accuracies are reported.

Method	# Params	CIFAR10	GTSRB	MNIST	RESISC45
Full-FT	100%	98.5	99.2	99.8	95.7
LoRA	0.3%	98.4	99.2	99.7	95.8
AdaLoRA	0.3%	98.6	99.3	99.6	95.8
SVFT	0.3%	98.7	99.5	99.6	95.0
VectorFit (Σ)	0.06%	<u>98.6</u>	<u>98.0</u>	<u>98.3</u>	<u>92.2</u>
VectorFit (<i>no avf</i>)	0.1%	99.0	99.6	99.0	94.4
VectorFit	0.1%	99.1	99.8	99.4	95.1

5.3. Natural Language Generation

We evaluate VectorFit on the XSum and CNN/DailyMail datasets using the ROUGE (1/2/L) metrics in Table 3. Despite a 33.3% higher relative parameter efficiency than the baselines, VectorFit consistently outperforms them on both datasets. Notably, VectorFit recovers 95% of Full-FT Rouge-L score with only 0.12% trainable parameters, compared to the baselines that recover 86% accuracy with 0.16% trainable parameters on the Xsum dataset. VectorFit’s performance surpasses Full-FT on CNN/Dailymail dataset, demonstrating superior efficiency and performance on complex tasks.

5.4. Image Classification

Table 4 showcases the results on image classification tasks. Our method surpasses Full-FT performance with only 0.1% trainable parameters. VectorFit achieves comparable results to the baselines while maintaining 80% higher relative parameter efficiency. Notably, VectorFit (Σ) demonstrates the highest parameter efficiency, with an average accuracy reduction of just 1.5% compared to Full-FT.

Table 5: Quantitative evaluation of Stable Diffusion v1.4 fine-tuned with PEFT methods using Dreambooth approach for Subject-driven Image generation. We evaluate subject fidelity using DINO and CLIP-I, and prompt fidelity using CLIP-T. Higher values indicate better performance across all metrics. # Params indicates the percentage of trainable parameters.

Method	# Params	DINO	CLIP-I	CLIP-T
Full-FT	100%	0.651	0.817	0.293
LoRA	0.04%	0.636	0.789	0.286
VectorFit	0.04%	0.642	0.796	0.289

5.5. Image Generation

Table 5 summarizes the results of personalized image generation using Dreambooth-style fine-tuning (Ruiz et al., 2023). The evaluation is conducted using three metrics: DINO, CLIP-I, and CLIP-T, as outlined in (Ruiz et al., 2023). Our method recovers an average DINO, CLIP-I, and CLIP-T score of 98.2% of Full-FT accuracy as opposed to 97.3% achieved by LoRA with 0.04% of trainable parameters. Fig-

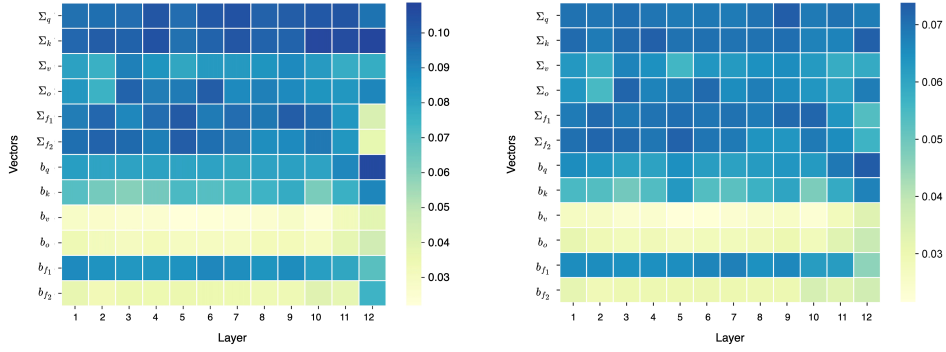


Figure 3: The training strength S_v of each trainable vector after fine-tuning of DeBERTaV3-base on the COLA dataset is shown for VectorFit without AVF (left) and with AVF (right). The x-axis represents the layer index, while the y-axis corresponds to different types of trainable vectors. The heatmaps show the regularization effect (overall lower S_v values) and the balanced training achieved with AVF.

ure 11 provides a visual comparison between Full-FT and VectorFit.

6. Discussion

6.1. Effect of Adaptive Vector Freezing

Proposition 1. *AVF has an effect comparable to that of dropout.*

Proof. Let n_u represent the total number of training/gradient update steps. The gradient of a vector v with respect to loss L is $\nabla_v L$. The expected gradient for the vector v per step without AVF is expressed as:

$$\mathbb{E}[\nabla_v L] = \frac{1}{n_u} \sum_{i=1}^{n_u} (\nabla_v L)_{[i]} \quad (6)$$

With n_f AVF steps, the training process can be divided into $n_f + 1$ gradient update intervals. Let p_j denote the probability that a vector v is frozen during the interval j . Let i_s and i_e be the temporary variables that denote the first and last gradient update step within each interval respectively. The expected gradient update per step for v under AVF can be expressed as:

$$\mathbb{E}_f[\nabla_v L] = \frac{1}{n_u} \sum_{j=1}^{n_f+1} \sum_{i=i_s}^{i_e} (1 - p_j) (\nabla_v L)_{[i]} \quad (7)$$

$$= \frac{1}{n_u} \left[\sum_{i=1}^{n_u} (\nabla_v L)_{[i]} - \sum_{j=1}^{n_f+1} \sum_{i=i_s}^{i_e} (p_j) (\nabla_v L)_{[i]} \right] \quad (8)$$

$$\mathbb{E}_f[\nabla_v L] = \mathbb{E}[\nabla_v L] - \frac{1}{n_u} \sum_{j=1}^{n_f+1} \sum_{i=i_s}^{i_e} (p_j) (\nabla_v L)_{[i]} \quad (9)$$

The second term of Eq. 9 captures the regularization effect of AVF. A similar analysis can be applied to dropout, demonstrating that AVF effectively minimizes co-adaptation. This effect is empirically validated in Figure 3.

6.2. Rank Analysis

Proposition 2. *Singular vector updates lead to high-rank incremental matrices.*

Ignoring the bias, the forward pass of VectorFit can be written as

$$y = U\Sigma V^T x \quad (10)$$

where x is the input for the current layer and y is the output of the layer before activation. We find the gradient of Σ with respect to loss L ($\nabla_{\Sigma} L$) during back-propagation, similar to (Ionescu et al., 2016) and (Hao et al., 2025):

$$\nabla_{\Sigma} L = (U^T V) \frac{\partial L}{\partial y} x^T \quad (11)$$

Here, $\frac{\partial L}{\partial y}$ is the partial derivative of L with respect to y , which can also be called as incoming-gradient. U and V are orthogonal matrices and hence $U^T V$ is also an orthogonal matrix. We interpret $\nabla_{\Sigma} L$ in Eq. 11 as orthogonal projection of input x transformed by incoming-gradient. Since orthogonal projection is rank-preserving, we hypothesize that the gradients of Σ are high-rank (and is a function of the input and incoming-gradient).

Proof. We empirically prove our hypothesis using the singular values of resultant incremental matrix Δ^* for the DeBERTaV3-base model fine-tuned on the COLA dataset using Full-FT and VectorFit. In Full-FT, Δ^* ,

$$\Delta^* = W_{init} - W_{final} \quad (12)$$

where $W_{init} \in \mathbb{R}^{d_r \times d_c}$ and $W_{final} \in \mathbb{R}^{d_r \times d_c}$ represent the pre-trained and fine-tuned weight matrices, respectively.

For VectorFit, Δ^* ,

$$\Delta^* = W_{init} - U\Sigma_{final}V^T \quad (13)$$

with U and V as the left and right singular matrices of W_{init} , and Σ_{final} as the singular vector after complete fine-tuning. Singular values of Δ^* from randomly selected layers are plotted in Figure 9 of Appendix D.4. The plots reveal that in Full-FT, a few singular values are significantly larger, while others are relatively small but non-zero, indicating that the incremental matrices are not purely low-rank.

Low-rank adaptation methods operate under the assumption that Δ^* consistently has a rank $r \ll \min(d_r, d_c)$. As a result, their gradient updates are restricted to a smaller subspace compared to Full-FT. The plots show that VectorFit successfully overcomes this drawback and is capable of achieving a full ranked Δ^* with rank $r = \min(d_r, d_c)$ while also achieving a higher parameter efficiency. In addition, training the bias vectors gives the model an extra degree of freedom to capture the distribution of the fine-tuning dataset.

We can also note that the singular values corresponding to VectorFit is higher than that of Full-FT for several layers. This means that the Δ^* of VectorFit has a higher concentrated energy and variance. This leads to a greater scaling and overall impact on the input vectors which helps in learning stronger internal representations for the data distribution.

6.3. Ablations on Choice of Vectors and AVF

This section presents the experiments that reveal the contribution of different vectors and the AVF mechanism to the performance of VectorFit. To this end, we explore 5 variants of VectorFit.

VectorFit (Σ_a): The singular vectors corresponding to $\{q, k, v, o\}$ are trained.

VectorFit (Σ): The singular vectors corresponding to $\{q, k, v, o, f_1, f_2\}$ are trained.

VectorFit ($\Sigma_a + b$): The singular vectors corresponding to $\{q, k, v, o\}$ and all the bias vectors are trained.

VectorFit (no avf): The singular vectors corresponding to $\{q, k, v, o, f_1, f_2\}$ and all the bias vectors are trained.

VectorFit: The singular vectors corresponding to $\{q, k, v, o, f_1, f_2\}$ and all the bias vectors are trained along with AVF.

Figure 4 presents the results of fine-tuning the DeBERTaV3-base model across five variants mentioned above on QA tasks. On the SQuADv1.1 dataset, the performance difference between VectorFit (*no AVF*) and VectorFit is 0.2%. On the more challenging SQuADv2.0 dataset, this difference increases to 0.5%, highlighting the critical role of AVF. Addi-

tionally, the average 1% performance gap between VectorFit (Σ_a) and VectorFit (Σ) underscores the importance of singular vectors associated with the fully connected modules (f_1 and f_2) in the transformer block. Lastly, the performance difference between VectorFit (Σ_a) and VectorFit ($\Sigma_a + b$) emphasizes the significance of training the bias vectors.

Figure 7 provides a similar analysis on the GLUE benchmark, yielding results consistent with the observations discussed earlier. Further examination of the training strength of various vectors for different VectorFit variants fine-tuned on the COLA dataset is included in Appendix D.1.

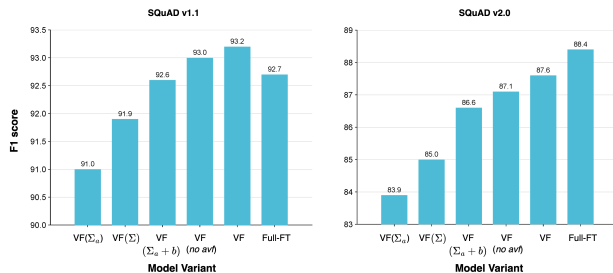


Figure 4: Ablation study about AVF and different trainable vectors configuration. We report the F1 scores for SQuAD v1.1 and SQuAD v2.0 datasets of QA task.

6.4. Limitations

Although VectorFit demonstrates exceptional performance with high parameter efficiency, the AVF mechanism’s effectiveness depends on careful hyperparameter selection, a challenge shared by comparable methods like AdaLoRA. To overcome this, we provide some heuristics for hyperparameter selection in Appendix C. Another limitation is that the number of trainable parameters is currently bounded, as no new parameterized weights are introduced. In future work, we aim to address this by exploring the parameterization of left and right singular matrices, potentially increasing the upper limit of trainable parameters and further enhancing the method’s flexibility and performance.

7. Conclusion

We introduce VectorFit, a novel PEFT approach that extracts meaningful singular vectors from weight matrices using SVD and adaptively trains the singular and bias vectors. This method enables high-rank and intrinsic knowledge-aware adaptation of pre-trained models, significantly enhancing both model performance and parameter efficiency. Through comprehensive experiments across diverse language and vision tasks, we demonstrate that VectorFit surpasses existing methods in terms of performance as a function of parameter efficiency. Also, utilizing VectorFit to fine-tune PFMs for downstream tasks is straightforward and cost effective. Additionally, we provide extensive the-

oretical and empirical insights into its operation to enable further research in this area. In future, we plan to conduct mathematical analysis of weight matrix transformations during fine-tuning, aiming to develop novel parameterization strategies beyond singular vectors and biases.

Broader Impact

Our approach facilitates the efficient customization of foundational models, which carries potential societal benefits and risks. By reducing the computational and parameter footprint, our method makes customization more cost-effective and accessible.

References

- Cheng, G., Han, J., and Lu, X. Remote sensing image scene classification: Benchmark and state of the art. *Proceedings of the IEEE*, 105(10):1865–1883, October 2017. ISSN 1558-2256. doi: 10.1109/jproc.2017.2675998. URL <http://dx.doi.org/10.1109/JPROC.2017.2675998>.
- Dehghani, M., Djolonga, J., Mustafa, B., Padlewski, P., Heek, J., and Gilmer, J. Scaling vision transformers to 22 billion parameters, 2023. URL <https://arxiv.org/abs/2302.05442>.
- Deng, L. The mnist database of handwritten digit images for machine learning research [best of the web]. *IEEE Signal Processing Magazine*, 29(6):141–142, 2012. doi: 10.1109/MSP.2012.2211477.
- Detrmers, T., Pagnoni, A., Holtzman, A., and Zettlemoyer, L. Qlora: efficient finetuning of quantized llms. In *Proceedings of the 37th International Conference on Neural Information Processing Systems, NIPS '23*, Red Hook, NY, USA, 2024. Curran Associates Inc.
- Ding, N., Lv, X., Wang, Q., Chen, Y., Zhou, B., Liu, Z., and Sun, M. Sparse low-rank adaptation of pre-trained language models. In *The 2023 Conference on Empirical Methods in Natural Language Processing*, 2023. URL <https://openreview.net/forum?id=jxgz7FEqWq>.
- Dosovitskiy, A., Beyer, L., Kolesnikov, A., Weissenborn, D., Zhai, X., Unterthiner, T., Dehghani, M., Minderer, M., Heigold, G., Gelly, S., Uszkoreit, J., and Houlsby, N. An image is worth 16x16 words: Transformers for image recognition at scale, 2021. URL <https://arxiv.org/abs/2010.11929>.
- Grattafiori, A., Dubey, A., Jauhri, A., and Pandey, A. The llama 3 herd of models. Technical report, Meta, <https://arxiv.org/abs/2407.21783>, 2024.
- Hao, Y., Cao, Y., and Mou, L. Flora: low-rank adapters are secretly gradient compressors. In *Proceedings of the 41st International Conference on Machine Learning, ICML'24*. JMLR.org, 2025.
- He, J., Zhou, C., Ma, X., Berg-Kirkpatrick, T., and Neubig, G. Towards a unified view of parameter-efficient transfer learning. In *International Conference on Learning Representations*, 2022. URL <https://openreview.net/forum?id=0RDcd5Axok>.
- He, P., Gao, J., and Chen, W. Debertav3: Improving deberta using electra-style pre-training with gradient-disentangled embedding sharing, 2023. URL <https://arxiv.org/abs/2111.09543>.
- Houlsby, N., Giurghi, A., Jastrzebski, S., Morrone, B., de Laroussilhe, Q., Gesmundo, A., Attariyan, M., and Gelly, S. Parameter-efficient transfer learning for NLP. *CoRR*, abs/1902.00751, 2019. URL <http://arxiv.org/abs/1902.00751>.
- Hu, E. J., Shen, Y., Wallis, P., Allen-Zhu, Z., Li, Y., Wang, S., Wang, L., and Chen, W. Lora: Low-rank adaptation of large language models, 2021. URL <https://arxiv.org/abs/2106.09685>.
- Ionescu, C., Vantzos, O., and Sminchisescu, C. Training deep networks with structured layers by matrix backpropagation, 2016. URL <https://arxiv.org/abs/1509.07838>.
- Koohpayegani, S. A., L, N. K., Nooralinejad, P., Kolouri, S., and Pirsiavash, H. NOLA: Compressing loRA using linear combination of random basis. In *The Twelfth International Conference on Learning Representations*, 2024. URL <https://openreview.net/forum?id=TjfXcDgvzk>.
- Kopiczko, D. J., Blankevoort, T., and Asano, Y. M. VeRA: Vector-based random matrix adaptation. In *The Twelfth International Conference on Learning Representations*, 2024. URL <https://openreview.net/forum?id=NjNfLdxr3A>.
- Krizhevsky, A. Learning multiple layers of features from tiny images. 2009. URL <https://api.semanticscholar.org/CorpusID:18268744>.
- Lester, B., Al-Rfou, R., and Constant, N. The power of scale for parameter-efficient prompt tuning. In Moens, M.-F., Huang, X., Specia, L., and Yih, S. W.-t. (eds.), *Proceedings of the 2021 Conference on Empirical Methods in Natural Language Processing*, pp. 3045–3059, Online and Punta Cana, Dominican Republic, November 2021. Association for Computational Linguistics. doi: 10.18653/v1/2021.emnlp-main.

243. URL <https://aclanthology.org/2021.emnlp-main.243/>.
- Lewis, M., Liu, Y., Goyal, N., Ghazvininejad, M., Mohamed, A., Levy, O., Stoyanov, V., and Zettlemoyer, L. BART: Denoising sequence-to-sequence pre-training for natural language generation, translation, and comprehension. In Jurafsky, D., Chai, J., Schluter, N., and Tetreault, J. (eds.), *Proceedings of the 58th Annual Meeting of the Association for Computational Linguistics*, pp. 7871–7880, Online, July 2020. Association for Computational Linguistics. doi: 10.18653/v1/2020.acl-main.703. URL <https://aclanthology.org/2020.acl-main.703/>.
- Li, J., Tang, T., Zhao, W. X., and Wen, J.-R. Pretrained language models for text generation: A survey, 2021. URL <https://arxiv.org/abs/2105.10311>.
- Li, R., allal, L. B., Zi, Y., Muennighoff, N., Kocetkov, D., Mou, C., Marone, M., Akiki, C., LI, J., Chim, J., Liu, Q., Zheltonozhskii, E., Zhuo, T. Y., Wang, T., Dehaene, O., Lamy-Poirier, J., Monteiro, J., Gontier, N., Yee, M.-H., Umapathi, L. K., Zhu, J., Lipkin, B., Oblokulov, M., Wang, Z., Murthy, R., Stillerman, J. T., Patel, S. S., Abulkhanov, D., Zocca, M., Dey, M., Zhang, Z., Bhattacharyya, U., Yu, W., Luccioni, S., Villegas, P., Zhdanov, F., Lee, T., Timor, N., Ding, J., Schlesinger, C. S., Schoelkopf, H., Ebert, J., Dao, T., Mishra, M., Gu, A., Anderson, C. J., Dolan-Gavitt, B., Contractor, D., Reddy, S., Fried, D., Bahdanau, D., Jernite, Y., Ferrandis, C. M., Hughes, S., Wolf, T., Guha, A., Werra, L. V., and de Vries, H. Starcoder: may the source be with you! *Transactions on Machine Learning Research*, 2023. ISSN 2835-8856. URL <https://openreview.net/forum?id=KoFOg41haE>. Reproducibility Certification.
- Li, X. L. and Liang, P. Prefix-tuning: Optimizing continuous prompts for generation. In Zong, C., Xia, F., Li, W., and Navigli, R. (eds.), *Proceedings of the 59th Annual Meeting of the Association for Computational Linguistics and the 11th International Joint Conference on Natural Language Processing (Volume 1: Long Papers)*, pp. 4582–4597, Online, August 2021. Association for Computational Linguistics. doi: 10.18653/v1/2021.acl-long.353. URL <https://aclanthology.org/2021.acl-long.353/>.
- Lingam, V., Neerkaje, A. T., Vavre, A., Shetty, A., Gudur, G. K., Ghosh, J., Choi, E., Dimakis, A., Bojchevski, A., and sujay sanghavi. SVFT: Parameter-efficient finetuning with singular vectors. In *2nd Workshop on Advancing Neural Network Training: Computational Efficiency, Scalability, and Resource Optimization (WANT@ICML 2024)*, 2024. URL <https://openreview.net/forum?id=DOUskwCqg5>.
- Liu, W., Qiu, Z., Feng, Y., Xiu, Y., Xue, Y., Yu, L., Feng, H., Liu, Z., Heo, J., Peng, S., Wen, Y., Black, M. J., Weller, A., and Schölkopf, B. Parameter-efficient orthogonal finetuning via butterfly factorization. In *The Twelfth International Conference on Learning Representations*, 2024. URL <https://openreview.net/forum?id=7NzggkEdGyr>.
- Nallapati, R., Zhou, B., dos Santos, C., Gülçehre, Ç., and Xiang, B. Abstractive text summarization using sequence-to-sequence RNNs and beyond. In Riezler, S. and Goldberg, Y. (eds.), *Proceedings of the 20th SIGNLL Conference on Computational Natural Language Learning*, pp. 280–290, Berlin, Germany, August 2016. Association for Computational Linguistics. doi: 10.18653/v1/K16-1028. URL <https://aclanthology.org/K16-1028/>.
- Narayan, S., Cohen, S. B., and Lapata, M. Don’t give me the details, just the summary! topic-aware convolutional neural networks for extreme summarization. In Riloff, E., Chiang, D., Hockenmaier, J., and Tsujii, J. (eds.), *Proceedings of the 2018 Conference on Empirical Methods in Natural Language Processing*, pp. 1797–1807, Brussels, Belgium, October-November 2018. Association for Computational Linguistics. doi: 10.18653/v1/D18-1206. URL <https://aclanthology.org/D18-1206/>.
- Paszke, A., Gross, S., Massa, F., Lerer, A., Bradbury, J., Chanan, G., Killeen, T., Lin, Z., Gimelshein, N., Antiga, L., Desmaison, A., Köpf, A., Yang, E., DeVito, Z., Raison, M., Tejani, A., Chilamkurthy, S., Steiner, B., Fang, L., Bai, J., and Chintala, S. *PyTorch: an imperative style, high-performance deep learning library*. Curran Associates Inc., Red Hook, NY, USA, 2019.
- Pfeiffer, J., Kamath, A., Rücklé, A., Cho, K., and Gurevych, I. Adapterfusion: Non-destructive task composition for transfer learning, 2021. URL <https://arxiv.org/abs/2005.00247>.
- Qiu, Z., Liu, W., Feng, H., Xue, Y., Feng, Y., Liu, Z., Zhang, D., Weller, A., and Schölkopf, B. Controlling text-to-image diffusion by orthogonal finetuning. In *Thirty-seventh Conference on Neural Information Processing Systems*, 2023. URL <https://openreview.net/forum?id=K30wTdIIYc>.
- Radford, A., Kim, J. W., Xu, T., Brockman, G., McLeavey, C., and Sutskever, I. Robust speech recognition via large-scale weak supervision, 2022. URL <https://arxiv.org/abs/2212.04356>.
- Rafailov, R., Sharma, A., Mitchell, E., Manning, C. D., Ermon, S., and Finn, C. Direct preference optimization: Your language model is secretly a reward model. In *Thirty-seventh Conference on Neural Information Processing*

- Systems*, 2023. URL <https://openreview.net/forum?id=HPuSIXJaa9>.
- Rajpurkar, P., Zhang, J., Lopyrev, K., and Liang, P. Squad: 100,000+ questions for machine comprehension of text, 2016. URL <https://arxiv.org/abs/1606.05250>.
- Rombach, R., Blattmann, A., Lorenz, D., Esser, P., and Ommer, B. High-resolution image synthesis with latent diffusion models. *2022 IEEE/CVF Conference on Computer Vision and Pattern Recognition (CVPR)*, pp. 10674–10685, 2021. URL <https://api.semanticscholar.org/CorpusID:245335280>.
- Ruiz, N., Li, Y., Jampani, V., Pritch, Y., Rubinstein, M., and Aberman, K. Dreambooth: Fine tuning text-to-image diffusion models for subject-driven generation, 2023. URL <https://arxiv.org/abs/2208.12242>.
- Shi, A. and DeVito, Z. Understanding gpu memory 1: Visualizing all allocations over time. URL <https://pytorch.org/blog/understanding-gpu-memory-1/>.
- Stallkamp, J., Schlipsing, M., Salmen, J., and Igel, C. Man vs. computer: Benchmarking machine learning algorithms for traffic sign recognition. *Neural Networks*, 32:323–332, 2012. ISSN 0893-6080. doi: <https://doi.org/10.1016/j.neunet.2012.02.016>. URL <https://www.sciencedirect.com/science/article/pii/S0893608012000457>. Selected Papers from IJCNN 2011.
- Sun, C., Wei, J., Wu, Y., Shi, Y., He, S., Ma, Z., Xie, N., and Yang, Y. Svfit: Parameter-efficient fine-tuning of large pre-trained models using singular values, 2024. URL <https://arxiv.org/abs/2409.05926>.
- Touvron, H., Lavril, T., Izacard, G., Martinet, X., Lachaux, M.-A., Lacroix, T., Rozière, B., Goyal, N., Hambro, E., Azhar, F., Rodriguez, A., Joulin, A., Grave, E., and Lample, G. Llama: Open and efficient foundation language models, 2023. URL <https://arxiv.org/abs/2302.13971>.
- Wang, A., Singh, A., Michael, J., Hill, F., Levy, O., and Bowman, S. R. Glue: A multi-task benchmark and analysis platform for natural language understanding, 2019. URL <https://arxiv.org/abs/1804.07461>.
- Wolf, T., Debut, L., Sanh, V., Chaumond, J., Delangue, C., Moi, A., Cistac, P., Rault, T., Louf, R., Funtowicz, M., Davison, J., Shleifer, S., von Platen, P., Ma, C., Jernite, Y., Plu, J., Xu, C., Scao, T. L., Gugger, S., Drame, M., Lhoest, Q., and Rush, A. M. Huggingface’s transformers: State-of-the-art natural language processing, 2020. URL <https://arxiv.org/abs/1910.03771>.
- Xu, C., Sun, Q., Zheng, K., Geng, X., Zhao, P., Feng, J., Tao, C., Lin, Q., and Jiang, D. WizardLM: Empowering large pre-trained language models to follow complex instructions. In *The Twelfth International Conference on Learning Representations*, 2024a. URL <https://openreview.net/forum?id=CfXh93NDgH>.
- Xu, Y., Xie, L., Gu, X., Chen, X., Chang, H., Zhang, H., Chen, Z., ZHANG, X., and Tian, Q. QA-loRA: Quantization-aware low-rank adaptation of large language models. In *The Twelfth International Conference on Learning Representations*, 2024b. URL <https://openreview.net/forum?id=WvFoJccp08>.
- Yu, L., Jiang, W., Shi, H., YU, J., Liu, Z., Zhang, Y., Kwok, J., Li, Z., Weller, A., and Liu, W. Metamath: Bootstrap your own mathematical questions for large language models. In *The Twelfth International Conference on Learning Representations*, 2024. URL <https://openreview.net/forum?id=N8N0hgNDRt>.
- Zhang, F., Li, L., Chen, J., Jiang, Z., Wang, B., and Qian, Y. Increlora: Incremental parameter allocation method for parameter-efficient fine-tuning, 2023a. URL <https://arxiv.org/abs/2308.12043>.
- Zhang, L., Zhang, L., Shi, S., Chu, X., and Li, B. LoRA-FA: Memory-efficient low-rank adaptation for large language models fine-tuning, 2024a. URL <https://openreview.net/forum?id=RbKThNNFxr>.
- Zhang, M., Chen, H., Shen, C., Yang, Z., Ou, L., Yu, X., and Zhuang, B. LoRAPrune: Pruning meets low-rank parameter-efficient fine-tuning, 2024b. URL <https://openreview.net/forum?id=9KVT1elqf7>.
- Zhang, Q., Chen, M., Bukharin, A., Karampatziakis, N., He, P., Cheng, Y., Chen, W., and Zhao, T. Adalora: Adaptive budget allocation for parameter-efficient fine-tuning, 2023b. URL <https://arxiv.org/abs/2303.10512>.
- Zi, B., Qi, X., Wang, L., Wang, J., Wong, K.-F., and Zhang, L. Delta-loRA: Fine-tuning high-rank parameters with the delta of low-rank matrices, 2024. URL <https://openreview.net/forum?id=FA04VS9QRV>.

A. Memory Usage

As discussed in Section 3.1, while retaining the left and right singular matrices increases the overall parameter count, the practical impact is minimal. Figure 5 compares the GPU memory usage of VectorFit and LoRA ($r = 1$) on the MNLI dataset using DeBERTaV3-base with full precision training. The figure demonstrates that both methods use comparable amounts of memory, where VectorFit requires approximately 200MB of additional memory using 0.08% of trainable parameters. This experiment was conducted on an Nvidia Titan XP GPU with 12GB of RAM.

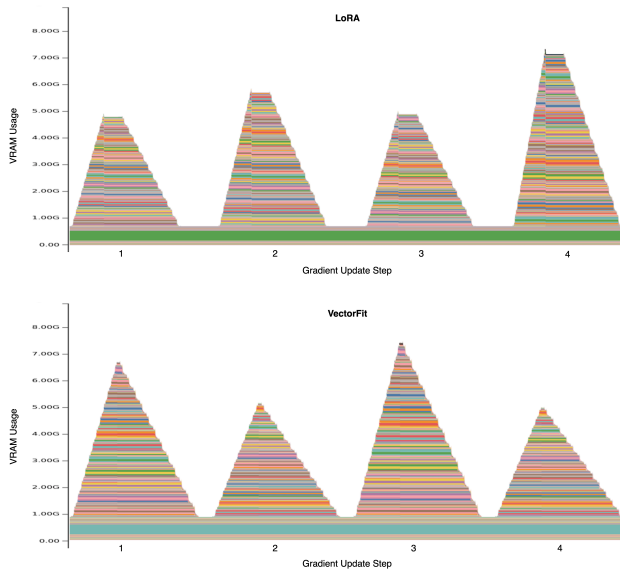


Figure 5: PyTorch memory trace (Shi & DeVito) comparison of 4 training steps for LoRA ($r = 1$) on the top and VectorFit on the bottom.

B. Training Speed

We fine-tune DeBERTaV3-base on the MNLI dataset with full precision and on the SQuAD v2.0 dataset with mixed precision training to assess the training speed of VectorFit, measured as the time required to train one epoch. Table 6 shows that VectorFit reduces training time by 17.5% on MNLI and 16.6% on SQuAD v2.0 compared to baseline. This improvement is due to VectorFit’s simpler computational graph compared to other methods, resulting in faster processing. This experiment was conducted on an Nvidia Titan XP GPU with 12GB of RAM.

Table 6: Comparison of practical training time.

Dataset	# Params	Method	Time / Epoch
MNLI	0.08%	LoRA	82 min
	0.08%	AdaLoRA	91 min
	0.08%	VectorFit	75 min
	0.07%	VectorFit ($\Sigma_a + b$)	71 min
	0.01%	VectorFit (Σ_a)	64 min
SQuAD v2.0	0.08%	LoRA	98 min
	0.08%	AdaLoRA	108 min
	0.08%	VectorFit	90 min
	0.07%	VectorFit ($\Sigma_a + b$)	84 min
	0.01%	VectorFit (Σ_a)	75 min

C. Implementation Details

This section outlines the implementation details of our method and the baselines used in various experiments. Most of our experiments were conducted on the NVIDIA A100(40G) GPU. We employ the AdamW optimizer with $\beta_1 = 0.9$ and $\beta_2 = 0.999$, no warmup, and no weight decay for all our experiments. For the AVF-related hyperparameters, we adopt the following values as a general guideline:

- t_i : Approximately 11 epochs’ worth of training steps to ensure proper warm-up for all trainable vectors.
- t_f : Approximately 1 epoch’s worth of training steps to allow for significant updates to the trainable vectors.
- $k \leq 5$: As this value is generally observed to yield the best performance with stable training.

C.1. Natural Language Understanding

Table 7 gives the hyperparameters used for each task in GLUE benchmark. We experimented using the following learning rates ($1e-2, 1e-3, 1e-4, 3e-4, 5e-4$) and observed that $1e-3$ works best for all tasks in GLUE.

Table 7: Hyperparameter setup of VectorFit for GLUE benchmark.

Dataset	learning rate	epochs	batch size	t_i	t_f	n_f	k
MNLI	$1e-03$	20	32	135000	10000	5	5
SST2	$1e-03$	30	32	23200	2100	10	5
COLA	$1e-03$	35	32	3000	200	5	5
QQP	$1e-03$	25	32	125100	11000	10	5
QNLI	$1e-03$	25	32	36000	3200	10	5
RTE	$1e-03$	50	32	800	70	27	5
MRPC	$1e-03$	50	32	1260	110	27	5
STSB	$1e-03$	50	32	1900	180	27	5

Table 8 presents the hyperparameters related to budget allocation of the baselines. d is the hidden dimension for the adapters, r is the rank of LoRA incremental weight matrices, and $b^{(T)}$ is the target budget of AdaLoRA. We use SVFT with random setting and $d = 2$.

Table 8: Budget setup of baselines for GLUE benchmark.

# Params	Houlsby Adapter (d)	Pfeiffer Adapter (d)	LoRA (r)	AdaLoRA ($b^{(T)}$)
1.2M	32	64	8	576
0.6M	16	32	4	288
0.3M	8	16	2	144

C.2. Question Answering

Table 9 gives the hyperparameters used for each dataset of QA task. We experimented using the following learning rates ($1e-2, 1e-3, 1e-4, 3e-4, 5e-4$) and observed that $1e-3$ works best for both datasets of QA task.

Table 9: Hyperparameter setup of VectorFit for question answering tasks.

Dataset	learning rate	epochs	batch size	t_i	t_f	n_f	k
Squad v1.1	$1e-03$	20	16	60700	5500	6	5
Squad v2.0	$1e-03$	20	16	90300	8200	6	5

Table 10 presents the hyperparameters related to budget allocation of the baselines.

Table 10: Budget setup of baselines for QA tasks.

# Params	Houlsby Adapter (d)	Pfeiffer Adapter (d)	LoRA (r)	AdaLoRA ($b^{(T)}$)	SVFT (d)
0.08%	4	8	1	72	1

C.3. Natural Language Generation

Table 11 gives the hyperparameters used for each dataset of NLG task. We experimented using the following learning rates ($1e-2$, $1e-3$, $1e-4$, $3e-4$, $5e-4$) and observed that $1e-3$ works best for both datasets of NLG task.

Table 11: Hyperparameter setup of VectorFit for natural language generation tasks.

Dataset	learning rate	epochs	batch size	t_i	t_f	n_f	k
XSum	$1e-03$	30	64	35070	3100	10	5
CNN/Dailymail	$1e-03$	30	64	31500	4400	10	5

Table 12 presents the hyperparameters related to budget allocation of the baselines used for experiments with Xsum and CNN/Dailymail datasets for NLG task.

Table 12: Budget setup of baselines for NLG tasks.

Houlsby Adapter (d)	Pfeiffer Adapter (d)	LoRA (r)	AdaLoRA ($b^{(T)}$)	SVFT (d)
8	16	2	144	2

C.4. Image Classification

Table 13 gives the hyperparameters used for each dataset of image classification task. We experimented using the following learning rates ($1e-2$, $1e-3$, $1e-4$, $3e-4$, $5e-4$) and the best performing learning rates are given in the table.

Table 13: Hyperparameter setup of VectorFit for image classification tasks.

Dataset	learning rate	epochs	batch size	t_i	t_f	n_f	k
CIFAR10	$1e-03$	20	128	3600	300	4	5
GTSRB	$1e-03$	20	128	1900	170	4	5
MNIST	$1e-02$	20	128	4300	350	4	5
RESISC45	$1e-02$	20	128	2300	200	4	5

For the baselines, we use LoRA with $r = 2$, AdaLoRA with $b^{(T)} = 144$, and SVFT with $d = 2$.

C.5. Image Generation

Dreambooth fine-tuning for various subjects in the dataset were done using prior preservation loss with the weightage varying between 0.5 to 1.0 depending on the subject. We use 300 class images for each subject, a learning rate of $5e - 5$, and a batch size of 4. We use the rank of 2 for fine-tuning with LoRA.

D. Additional Experiments

D.1. Training Strength Ablation

Figure 6 shows the training strength heatmap of various trainable vectors for different variants of VectorFit. We can observe that VectorFit with AVF (top-right) achieves the most equitable training possible among the trainable vectors and hence maintains an overall lower training strength. We can also observe that as the number of trainable vectors is reduced, the training strength of the vectors increases to make up for the reduced number of trainable parameters.

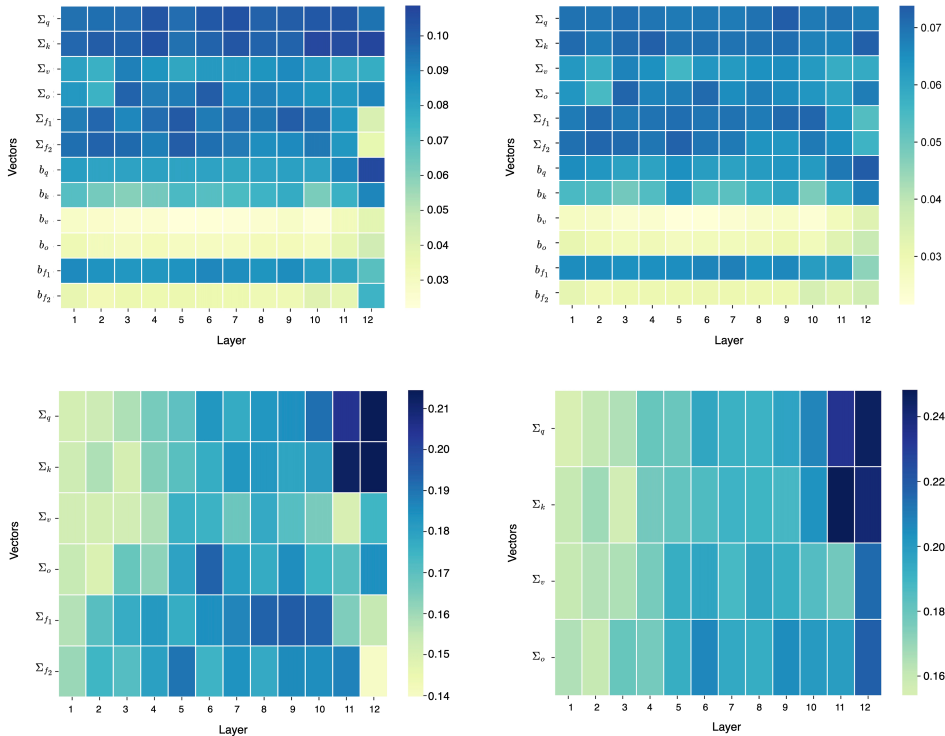


Figure 6: The training strength S_v of each trainable vector after fine-tuning of DeBERTaV3-base on the COLA dataset is shown for VectorFit without AVF (top-left), VectorFit with AVF (top-right), VectorFit (Σ) (bottom-left), and VectorFit (Σ_a) (bottom-right). The x-axis represents the layer index, while the y-axis corresponds to different types of trainable vectors.

D.2. NLU Tasks Ablation

Figure 7 shows the ablation graphs for the GLUE benchmark with all five variants of our method. The graphs show the efficacy of AVF where VectorFit with AVF gives a higher performance on all the datasets.

VectorFit

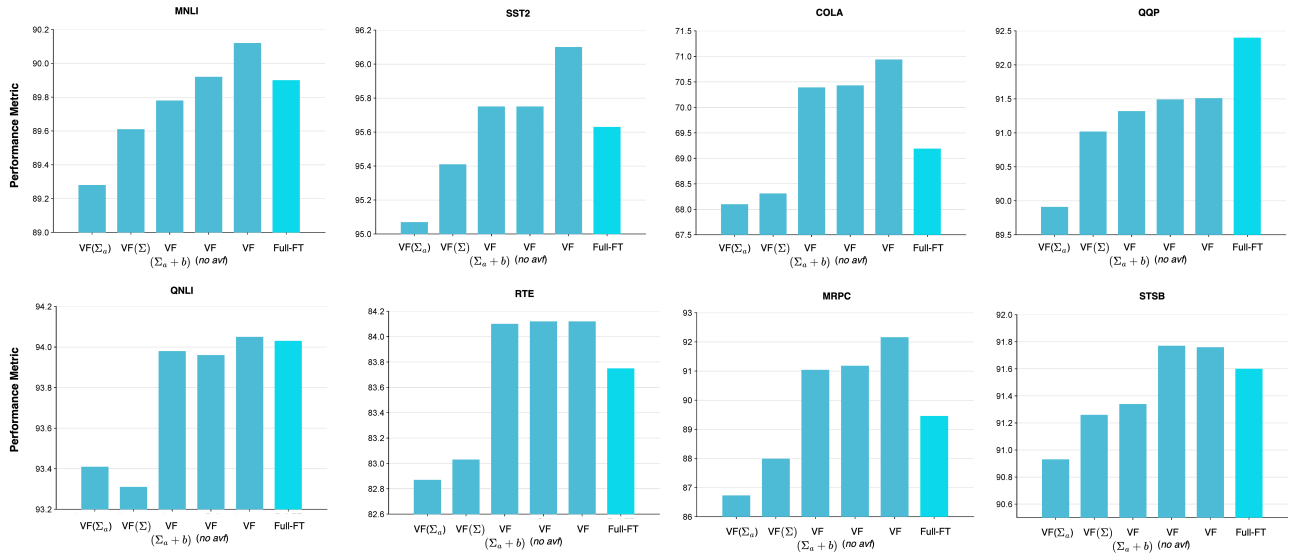


Figure 7: Ablation study about AVF and different trainable vectors configuration on the GLUE benchmark. We report the matched accuracy for MNLI, Matthew’s correlation for CoLA, Pearson correlation for STS-B, and accuracy for the other tasks.

D.3. QA Tasks Ablation

Table 14 presents the performance of various VectorFit variants. Notably, the most parameter-efficient version, VectorFit(Σ_a), which uses only 0.01% of trainable parameters, achieves up to 98% of the F1 score obtained with Full-FT.

Table 14: Ablation study on QA.

Model	# Params	Squad v1.1 (EM/F1)	Squad v2.0 (EM/F1)
VectorFit (Σ_a)	0.01%	83.8/91.0	80.2/83.9
VectorFit (Σ)	0.02%	84.9/91.9	81.6/85.0
VectorFit ($\Sigma_a + b$)	0.07%	86.4/92.6	83.7/86.6
VectorFit (no avf)	0.08%	86.7/93.0	84.2/87.1
VectorFit	0.08%	87.0/93.2	84.4/87.6

D.4. Rank Analysis Continued

Figure 9 presents the singular value distributions of the Δ^* matrices discussed in Section 6.2. For the DeBERTaV3-base model, each singular vector is 768-dimensional, and all 768 singular values are plotted. The graphs reveal that Δ^* for Full-FT is not inherently low-rank, as even the smallest singular values remain non-zero for many weight matrices. Additionally, the plots demonstrate that VectorFit achieves high-rank adaptation, closely approximating Full-FT for several weight matrices. Figure 8 shows the singular values of Δ^* of ViT-base model fine-tuned with VectorFit on CIFAR10 dataset.

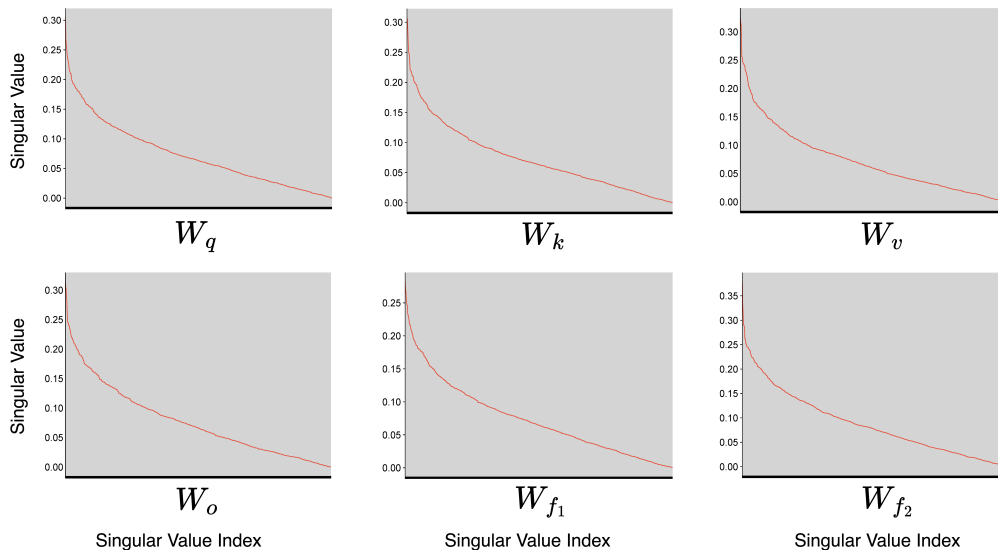


Figure 8: Singular value graphs of Δ^* for all the modules of a randomly picked layer (layer 6) of ViT-base model fine-tuned with VectorFit on CIFAR10 dataset. X-axis represents the singular value position/index and Y-axis represents the singular value.

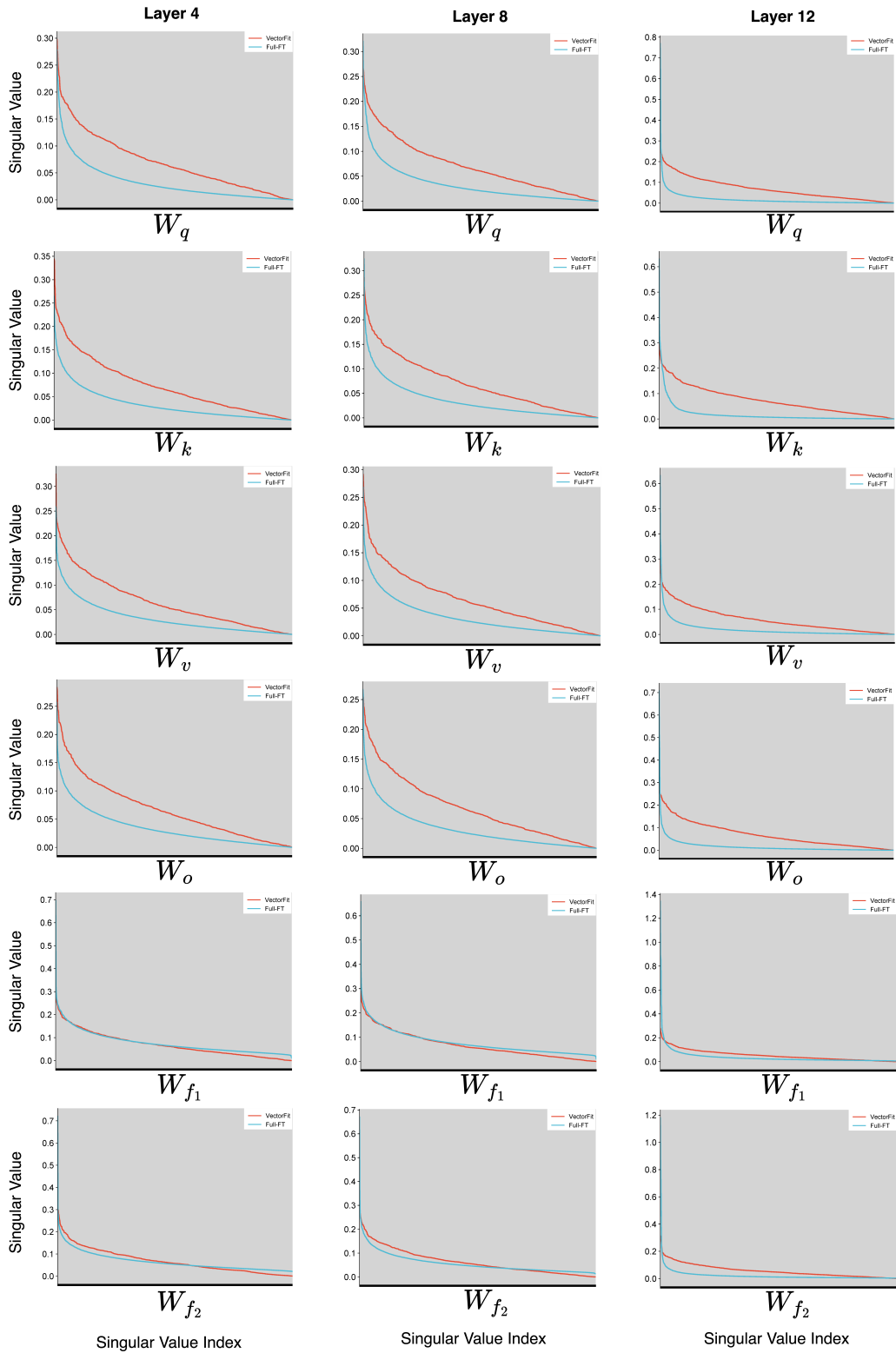


Figure 9: Singular value graphs of Δ^* for all the modules of randomly picked layers in case of VectorFit and Full-FT. X-axis represents the singular value position/index and Y-axis represents the singular value.

D.5. Weight Transformation During VectorFit Fine-Tuning

The heatmap of variation of the first 64 singular values before and after full fine-tuning in each singular vector of randomly selected layers is displayed in Figure 10. This depicts the weight matrix’s stretching in its multi-dimensional hyper-space. It should be noted that upon fine-tuning, even the least significant singular directions might become the principal singular directions. This shows that VectorFit is highly expressive.

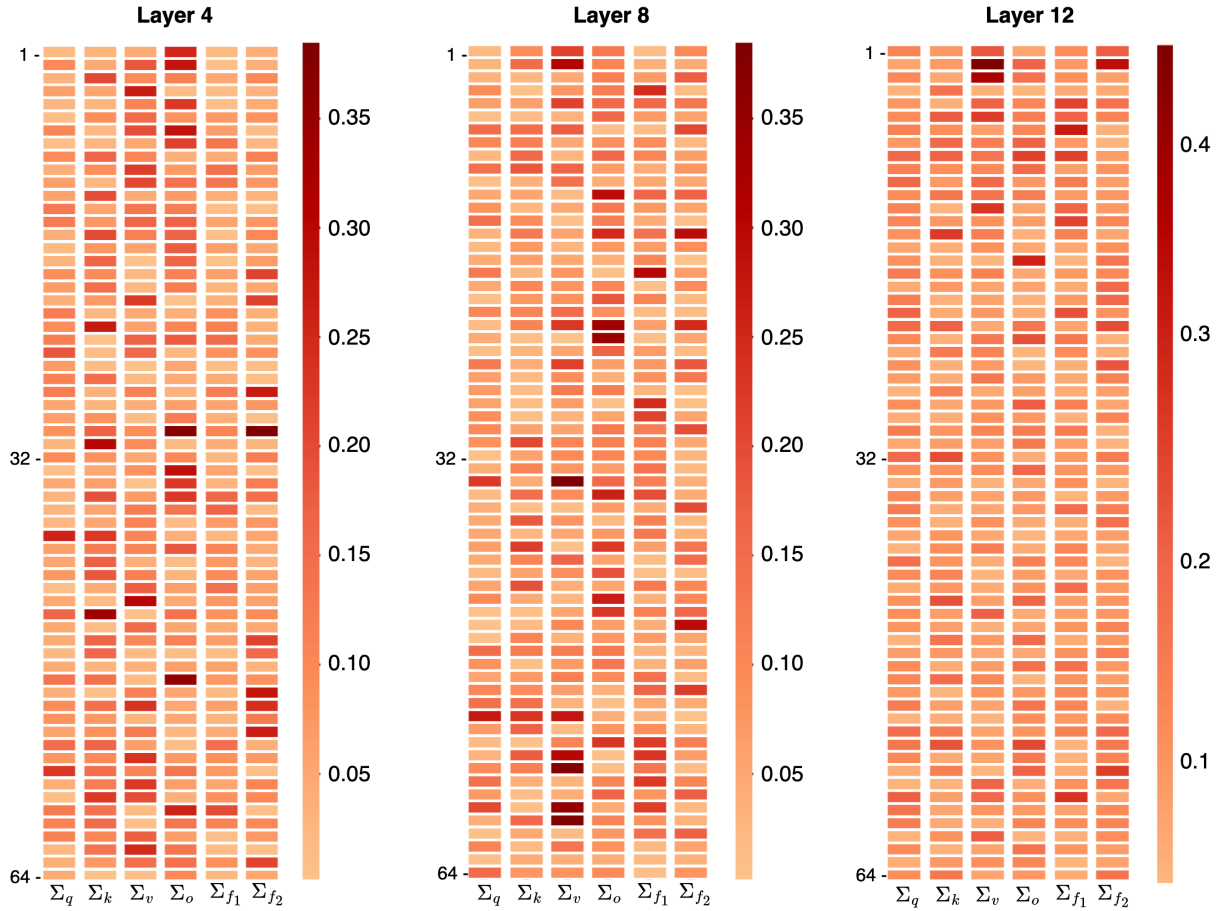


Figure 10: Heatmap representing the variations in first 64 singular values of different singular vectors before and after fine-tuning. The heatmaps are generated with randomly picked layers of DeBERTaV3-base model fine-tuned using VectorFit on COLA dataset.

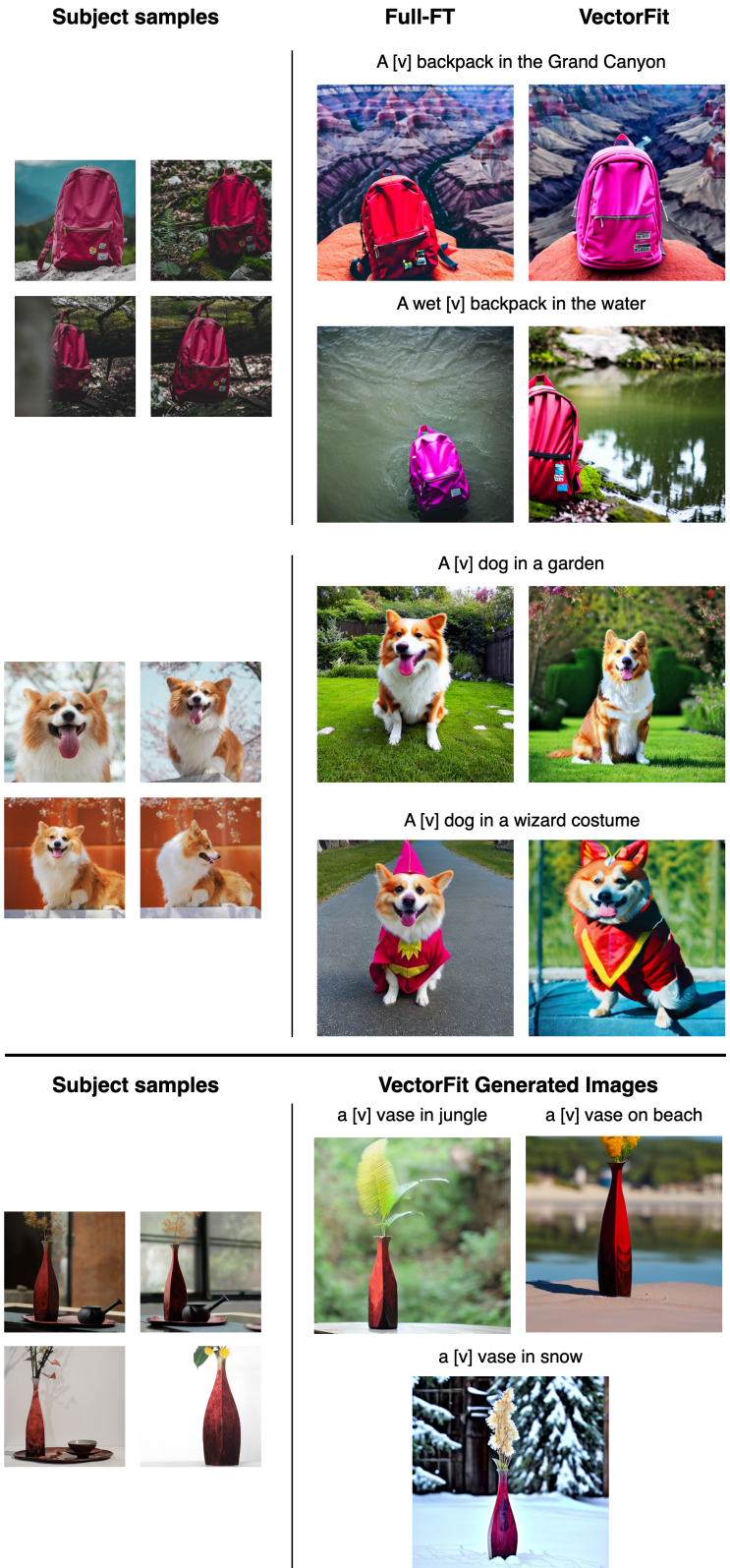


Figure 11: Visual comparison of images generated by Stable Diffusion v1.4 fine-tuned with VectorFit and Full-FT methods using Dreambooth approach for Subject-driven Image generation.